Combined Multireference Configuration Interaction/ Molecular Dynamics Approach for Calculating Solvatochromic Shifts: Application to the $n_O \rightarrow \pi^*$ Electronic Transition of Formaldehyde

ZongRong Xu and Spiridoula Matsika*

Department of Chemistry, Temple University, Philadelphia, Pennsylvania 19122

Received: July 17, 2006; In Final Form: August 30, 2006

A combined quantum mechanics/molecular mechanics method is described here for considering the solvatochromic shift of excited states in solution. The quantum mechanical solute is described using high level multireference configuration interaction methods (MRCI), while molecular dynamics is used for obtaining the structure of the solvent around the solute. The electrostatic effect of the solvent is included in the quantum description of the solute in an averaged way. This method is used to study solvent effects on the $n_O \rightarrow \pi^*$ electronic transition of formaldehyde in aqueous solution. The effects of solute polarization, basis sets, and dynamical correlation on the solvatochromic shift, and on dipole moments, have been investigated.

1. Introduction

The solvent effect on excited states is important in UV/visible spectra and in the photochemistry and photophysics of chemical systems in the condensed phase. Solvatochromic shifts, shifts of the absorption bands due to the solvent, provide an important experimental technique for probing solute−solvent interactions, and they have been studied extensively. Describing theoretically solvatochromic shifts is a challenging task since it involves two problems that are difficult to model even with modern quantum mechanical methods: the accurate description of solvent effects and the accurate description of excited electronic states.

There are different levels of sophistication for including solvent effects in the theoretical treatment of molecular systems. The different models can be broadly categorized into two types: the continuum models[1−3] and the discrete models.[4−13] In the continuum models, the solvent is represented by a dielectric continuum, and one can concentrate one's attention on the solute molecule. The advantage of dielectric continuum models is that they are fast enough so high level quantum mechanical methods can be used for the solute. Due to the microscopic structure of the solvent being neglected, however, one cannot take into account the influence of specific interactions. Alternatively, discrete models provide a very detailed description of the solvent structure. In this category classical simulations based on molecular dynamics (MD)[14,15] or Monte Carlo (MC)[16] simulations are used to obtain configurations describing the solvent structure around the solute, which are then combined with quantum mechanical calculations for the solute. These QM/MM or QM/MC methods have been known for a long time. Initially they employed semiempirical methods for the quantum mechanical (QM) segment or they focused on the ground-state properties, but soon contributions focusing on the study of the solvent effect on excited states appeared.[8−13] In recent years QM/MM approaches have been described with much higher sophistication on the quantum description of the excited states, by using ab initio multiconfigurational self-consistent field (MCSCF) or coupled cluster based approaches.[17−20]

The multireference configuration interaction (MRCI) method is a very accurate method for the description of excited states, mixed character (multireference) states, and distorted geometries. This method has been used extensively for the accurate description of excited states of molecules and radicals in the gas phase. The availability of analytic gradients for the MRCI wave functions has made this method optimum for studies of excited states away from the Franck Condon region and in nonadiabatic processes.[21−29] An efficient way to incorporate solvent effects within the MRCI methodology will provide a highly accurate way to study solvated excited states.

The aim of this work is to present an implementation of a QM/MM approach using MCSCF and MRCI ab initio methods. The method combines a high-level MRCI description for the solute and a detailed description of the solvent structure obtained from molecular dynamics simulations using a classical force field. In a usual QM/MM calculation the excitation energy shift can be obtained by computing the excitation energy for each solvent configuration first and then calculating the average value of excitation energies over many solvent configurations. Executing this scheme requires N times QM computations in order to obtain the averaged value of excitation energies over N solvent configurations, so for a statistically converged result hundreds or thousands of QM calculations are needed. Although this is possible using semiempirical QM calculations, it becomes extremely computationally intensive when an MRCI quantum mechanical method is used. To reduce the number of quantum mechanical calculations mean field approaches have been developed in the past.[19,30−38] In the present work a mean field approach based on Aguilar and co-workers' method[19,34−38] will be used to reduce the number of ab initio calculations needed. In this approach initially several molecular dynamics (MD) calculations are performed where the charges of the solute are taken from an initial QM calculation. Instead of performing a QM calculation for each solvent configuration, however, the average electrostatic potential of all configurations is calculated and introduced into the solute Hamiltonian. In this way only very few quantum calculations are needed. In this work the polarization of the solute due to the solvent is taken into account but not the polarization of the solvent.

* Corresponding author e-mail: smatsika@temple.edu.

10.1021/jp064520d CCC: $33.50
Published on Web 10/11/2006

This method is implemented into the COLUMBUS suite of ab initio programs[39−42] which is interfaced with the TINKER package for molecular dynamics simulations.[43] COLUMBUS includes a graphical unitary group approach (GUGA) based MRCI[39] with analytic gradients and is designed for the accurate description of electronically excited states.

The MRCI/MD approach is applied to the study of solvent effects on the $n_O \rightarrow \pi^*$ electronic transition in formaldehyde. The solvatochromic effect on the S_1 state of formaldehyde has been studied using many solvation models and provides a good benchmark for comparison between the different theoretical models.[12,17,19,20,31,32,44−50] For this type of transition ($n_O \rightarrow \pi^*$) in a polar solvent, like water, the electrostatic component is dominant.[20] Here the solvent effects on dipole moments and excitation energies are presented. The effects of basis sets, dynamical correlation, and the choice of partial charges on the atoms will be discussed. Finally comparisons with other theoretical and experimental results will be given.

The following section describes the general methodology, along with details about the MD simulations and ab initio calculations used. The results derived from application of the method to formaldehyde are discussed in section 3, and conclusions complete the paper.

2. Methodology

The QM/MM theory involves coupling between a quantum and a classical system. The Hamiltonian for the whole system may be partitioned as

$$\hat{H} = \hat{H}_{\mathrm{QM}} + \hat{H}_{\mathrm{MM}} + \hat{H}_{\mathrm{QM/MM}} \tag{1}$$

with terms that correspond to the quantum part, $\hat{H}_{\mathrm{QM}}$, the classical part, $\hat{H}_{\mathrm{MM}}$, and the interaction between them, $\hat{H}_{\mathrm{QM/MM}}$. When studying solvent effects, the quantum part involves only the solute molecule, while the classical part includes the solvent molecules. The quantum mechanical approach chosen to describe the solute system here is an MCSCF followed by an MRCI approach in order to best describe excited states. The solvent is represented by classical mechanics using an appropriate force field. The coupling between the two parts is given, in atomic units, in general by

$$\hat{H}_{\mathrm{QM/MM}} = \hat{H}^{\mathrm{el}} + \hat{H}^{\mathrm{vdW}} + \hat{H}^{\mathrm{pol}} \tag{2}$$

with

$$\hat{H}^{\mathrm{el}} = -\sum_{iM} \frac{Q_M}{|r_i - R_M|} + \sum_{\alpha M} \frac{Z_\alpha Q_M}{|R_\alpha - R_M|} \tag{3}$$

$$\hat{H}^{\mathrm{vdW}} = \sum_{\alpha M} 4\epsilon_{\alpha M} \left\{ \left(\frac{\sigma_{\alpha M}}{|R_\alpha - R_M|} \right)^{12} - \left(\frac{\sigma_{\alpha M}}{|R_\alpha - R_M|} \right)^{6} \right\} \tag{4}$$

where r_i are electronic coordinates, and R_α and R_M are coordinates of the nuclei of the solute and the classical atoms of the solvent, respectively. $\hat{H}^{\mathrm{el}}$ represents the electrostatic interactions between the electrons and nuclei with atomic number Z_α of the quantum molecule with the charges Q_M on the atoms of the solvent, $\hat{H}^{\mathrm{vdW}}$ represents the van der Waals interactions, and $\hat{H}^{\mathrm{pol}}$ is the interaction of the polarized solvent with the solute. Including $\hat{H}^{\mathrm{el}}$ into the quantum mechanical Hamiltonian accounts for the electrostatic interaction and may account for the polarizability of the solute due to the solvent.

The last term, $\hat{H}^{\mathrm{pol}}$, is more complicated to account for. To include this term, a polarizability has to be assigned to every classical molecule, and a dipole moment is induced by the electric field of the solute. The interaction of the induced dipoles with the field gives the polarization term. This procedure has to be solved self-consistently for the ground and excited states. Previous work[20,49] has shown this effect to change the shift by about 100 or 500 cm^{-1}. Kongsted and co-workers,[20] who found an effect of about 500 cm^{-1}, concluded that the major effect was due to the different solvent structure obtained from the MD calculations including polarization and not due to the incorporation of $\hat{H}^{\mathrm{pol}}$ into the quantum mechanical operator. In that work[20] including the polarization term explicitly into the quantum calculation only changed the shift by 78 cm^{-1}. In the present study the solvent polarizability is not included in the Hamiltonian, although future work will investigate its effect. Polarizability of the water, however, due to the other water molecules is implicitly accounted for by using a water force field that has partial charges that reproduce the solvated water dipole moment.

The electronic energies and wave functions of the solute are obtained by solving the effective Schrödinger equation with Hamiltonian $\hat{H}_{\mathrm{QM}} + \hat{H}_{\mathrm{QM/MM}}$. Since in this work the $\hat{H}^{\mathrm{pol}}$ term is neglected and $\hat{H}^{\mathrm{vdW}}$ is independent of the solute electronic coordinates, only the first one-electron term depends on the electronic coordinates and can be easily incorporated into the quantum mechanical codes. Including this term the corresponding nonrelativistic Hamiltonian operator will have the form, in second-quantized language

$$\hat{H}_{\mathrm{QM}} + \hat{H}_{\mathrm{QM/MM}} = \sum_{pq} \left\langle p \left| \hat{h}^0 + \sum_M \frac{Q_M}{|R_M - r|} \right| q \right\rangle \hat{E}_{\mathrm{pq}} + \frac{1}{2} \sum_{pqrs} \langle pq|\, rs\rangle (\hat{E}_{\mathrm{pq}} \hat{E}_{\mathrm{rs}} - \delta_{\mathrm{qr}} \hat{E}_{\mathrm{ps}}) + \hat{H}^{\mathrm{nel}} \tag{5}$$

where $\hat{H}^{\mathrm{nel}}$ includes the electronic-coordinate-independent terms. The terms $\langle p|\hat{h}^0 + \Sigma_M Q_M/|R_M - r||q\rangle$ and $\langle pq|rs\rangle$ are one- and two-electron integrals, respectively, over spatial orbitals, and $\hat{E}_{\mathrm{pq}}$ are the generators of the unitary group defined in terms of creation and annihilation operators

$$\hat{E}_{\mathrm{pq}} = \hat{a}^\dagger_{\mathrm{p}\alpha} \hat{a}_{\mathrm{q}\alpha} + \hat{a}^\dagger_{\mathrm{p}\beta} \hat{a}_{\mathrm{q}\beta} \tag{6}$$

The extra term $\Sigma_M \langle p|Q_M/|R_M - r||q\rangle$ is included in the QM calculations, where Q_M can be partial charges on the classical atoms or fitted partial charges, as will be described below.

In a usual QM/MM approach an MD calculation produces configurations of the solvent molecule around the solute, and for each configuration a QM calculation is run with the Hamiltonian including the $H_{\mathrm{QM/MM}}$ interaction. This approach requires thousands of QM calculations. In the average approach introduced by Aguilar and co-workers,[19,34,38] and being used here, the electrostatic potential for all configurations is averaged, and the average potential is introduced into the Hamiltonian. The average potential is fitted to a Coulomb potential produced by charges placed on a grid. So the final form introduced into the Hamiltonian is the same as H^{el} with the charges now being fitted charges placed on a grid rather than atomic charges on the atoms. In detail, the procedure begins by performing one quantum calculation for the solute molecule in the gas phase. The in vacuo solute geometry and partial charges are then used as input in the MD simulation. The quantum mechanical determination of the partial charges used here is based on the CHELPG algorithm[51,52] and is described in section 2.1. Once the structure of the solvent around the solute is obtained from the MD data, the averaged solvent electrostatic potential (ASEP)

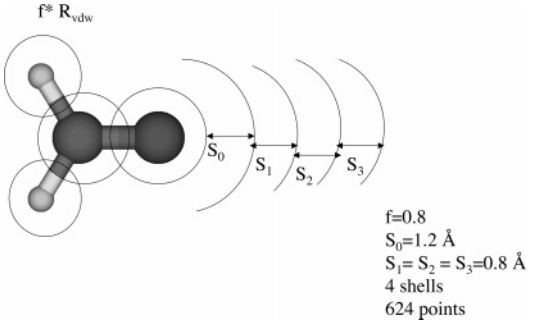

Figure 1. The parameters defining the grid point to represent the ASEP.

is determined, and then a set of electric charges $\{Q_X\}$ is produced at some chosen grid points $\{X\}$ by a least-squares fitting procedure which gives the best charges that can represent ASEP as an effective Coulomb potential, $\Sigma_X\langle p|Q_X/|R_X - r||q\rangle$. Details of the fitting procedure are given in section 2.2. The new set of charges is introduced into the QM Hamiltonian as one-electron terms. The electronic wave functions of the solute in solution is obtained by solving the associated effective Schrödinger equation.

If the polarizability of the solute is ignored, then the process is completed by introducing the perturbation attributable to the charges into the molecular Hamiltonian and solving the associated Schrödinger equation as described above. To account for the polarizability of the solute though we use the above procedure only as the first iteration. After obtaining the electronic wave functions of the solute in the presence of the solvent, the output of this calculation, especially the atomic charges, become the input of the next MD simulation. This process is repeated until statistical convergence in the solute atomic charges is achieved. This iterative procedure provides the polarization of the solute in the presence of the solvent.

2.1. Fitting the ASEP. The average electrostatic potential (ASEP) produced by many configurations of the solvent is represented by an effective electrostatic potential where the charges are determined by least-squares fitting, based on Sánchez's et al.[34] approach. First a solute cavity is defined in terms of intersecting spheres centered on the solute atoms. The cavity radius is taken as *f*-times the van der Waals radius of each atom. Two different grids are needed in this procedure. The first grid is used to calculate the ASEP felt by the solute in the presence of the solvent. These grid points were chosen inside the solute cavity in a rectangular three-dimensional grid. In this work, 104 points were chosen from a 11 × 11 × 11 mesh centered at the molecular geometric center, where grid points were separated by 0.5 Å. The second grid is the grid of points where the effective fitted charges are placed, and this grid surrounds the solute molecule. The fitted charges are placed in several shells around this van der Waals surface retaining its shape, as shown in Figure 1. The arrangement of the grid points is chosen so as to reproduce the solvent induced electrostatic potential of individual configurations. Least-squares fitting[51] is used to fit the charges placed on the grid into the electrostatic potential. This can be done for each individual configuration to find out the best fitting parameters: the scaling *f* value, the interval between the first shell and the van der Waals surface, s_0, and the interval between second shell and the van der Waals surface, s_1, and so on. Figure 1 displays in a diagram the definition of these parameters. In our fittings, $f = 0.8$, $s_0 = 1.20$ Å, and $s_1 = s_2 = s_3 = 0.8$ Å were found to be the best parameters for the system considered. Since we are interested in the energy shifts, the set of parameters was optimized for several chosen uncorrelated configurations so that the energy shifts derived from the fitting matched the energy shifts produced from the solvent configurations. The error from the fitting is estimated from these tests to be less than 100 cm^{-1}. The number of grid points on each shell should be limited to prevent divergence in the potential. The total number of grid points with four shells is 624. Note that before the fitting procedure, each configuration chosen was translated and rotated into a fixed principal axis system setup by the solute geometry to make all the solvent coordinates refer to a reference system centered on the solute mass center with the axes lying along the axes of inertia of the solute.

2.2. Atomic Charges Derived from Electrostatic Potential. The determination of atomic charges from quantum calculations is a key step in this procedure. It is generally believed that partial charges derived from Mulliken population analysis are not appropriate as atomic charges. Chirlian and Francl[51] developed a scheme (called CHELP) to derive atomic charges by fitting them to reproduce the molecular electrostatic potential (MESP), and the scheme was further modified by Breneman and Wiberg.[52] Along the same way, we developed a code, ESPCHG, to calculate the MESP and to derive atomic charges from MRCI wave functions and densities. First the one electron integrals of the form

$$\left\langle p\left|\frac{1}{|R_X - r|}\right|q\right\rangle \tag{7}$$

are computed at chosen grid point X around the molecular van der Waals surface, between MOs ϕ_p and ϕ_q, and collected in a matrix $[1/|R_X - r|]$. Then, the electrostatic potential due to interactions with electrons, V_e, is computed at point X by

$$V_e(R_X) = \mathrm{Tr}\gamma\left[\frac{1}{|R_X - r|}\right] \tag{8}$$

where γ is the one-electron reduced density matrix having elements, in MRCI formalism[53]

$$\gamma_{pq} = \sum_{IJ} c_I c_J \langle \Phi_I|\, \hat{E}_{pq}|\Phi_J\rangle \tag{9}$$

Φ_I and c_I are the configuration state functions (CSFs) and the corresponding CI coefficients, respectively ($\Psi^{MRCI} = \Sigma_I c_I \Phi_I$). The total MESP is the algebraic sum of V_e and the pure nuclear electrostatic potential V_N. Finally, the fitted atomic charges are derived from this potential by a least-squares fitting procedure. Two algorithms have been employed. One employs the Lagrange mutiplier method to introduce the constraint that the net molecular charge equals the algebraic sum of atomic charges and leads to a matrix equation with the form $\mathbf{AQ} = \mathbf{B}$.[51] The second scheme introduced by Williams yields a similar matrix equation, however, smaller in size.[54] There are also two practical algorithms for solving the resultant equations: inversion of **A** to find the charge array $\mathbf{Q} = \mathbf{A^{-1}B}$ or use of singular value decomposition as solver. The algorithm has been tested by comparing the charges obtained from an SCF calculation with those derived from CHELPG as implemented in the Gaussian suite of programs.[55]

2.3. Molecular Dynamics Simulation. The MD simulations have been performed using the TINKER molecular dynamics package.[43] A cubic box of side 18.6216 Å containing 210 rigid water molecules and a rigid formaldehyde molecule at the temperature of 298 K and constant volume was used. The minimum image periodic boundary conditions[16] have been

TABLE 1: Partial Charges in au on the Atoms of H_2CO Derived from the MESP Using Different ab Initio Methods[a]

method	Q_C	Q_O	Q_H	μ_g (D)
SCF/cc-pvdz	0.462	−0.462	0.000	2.66
SCF/cc-pvtz	0.443	−0.470	0.013	2.77
MRCI(4,3)/cc-pvtz	0.376 (0.447)	−0.394 (−0.481)	0.009 (0.017)	2.34
MRCI(6,4)/cc-pvtz	0.377 (0.451)	−0.394 (−0.486)	0.009 (0.018)	2.34
MRCI(4,3)/6-31++G**	0.468 (0.566)	−0.440 (−0.554)	−0.001 (−0.006)	2.48
MRCI(4,3)/aug-cc-pvtz	0.390 (0.489)	−0.406 (−0.510)	0.008 (0.010)	2.40

[a] Charges correspond to gas-phase H_2CO, while charges in parentheses correspond to the solvated H_2CO. The dipole moment derived from the gas-phase charges is also shown.

applied, and the particle mesh Ewald[56−58] has been used for charge interactions.

The rigid formaldehyde molecule has a geometry taken from the MP2/cc-pvtz calculations, R(CO) = 1.210 Å, R(CH) = 1.101 Å, ∠HCO = 121.9°, ∠HCH = 116.1°. These values are kept fixed in the MD simulation, since this work focuses on the vertical electronic transition. The force field for water uses the flexible SPC parameters[59] where the 6−12 type Lennard-Jones potential parameters are (σ_O,ϵ_O) = (3.1656 Å, 0.1554 kcal/mol), and the corresponding parameters for H are zero. The partial charges on the atoms O and H of water are $Q_O = -0.8200$ and $Q_H = 0.4100$, respectively. The initial atomic charges of formaldehyde were taken from the ab initio MRCI calculations using the code ESPCHG. These charges are given in Table 1 for the different ab initio models used in this work. Literature values were used for formaldehyde molecular mechanics parameters[20,60] where the 6−12 type Lennard-Jones potential parameters are (σ_O,ϵ_O) = (2.8200 Å, 0.2000 kcal/mol), (σ_C,ϵ_C) = (3.2960 Å, 0.1200 kcal/mol), and (σ_H,ϵ_H) = (2.7440 Å, 0.0100 kcal/mol). The original $\sigma_O = 2.85$ Å had been slightly adjusted to match our atomic charge on O by considering the empirical relationship[61]

$$\sigma = \sigma' \exp[a(Q - Q')] \tag{10}$$

where the constant $a = -0.0894$ for O is determined from atomic radii of O and O^{2-} based on the ab initio van der Waals radii of Badenhoop and Weinhold.[62] For the mixed 6−12 type L−J potential parameters (σ_{IJ},ϵ_{IJ}), the Lorentz−Berthelot mixing rules[63] were applied: $\sigma_{IJ} = 1/2\ (\sigma_I + \sigma_J)$, $\epsilon_{IJ} = \sqrt{\epsilon_I \epsilon_J}$.

The MD simulation was carried out with a time step of 2.0 fs and run for more than 1 ns. During the run the temperature and pressure are monitored by adjusting the coupling strength parameters to couple the system with external thermal and pressure baths. The total energy fluctuation should be very small. Upon the production phase, after the atomic charges were converged, the dynamics output was collected. For studying the blueshift, around 2000 configurations were collected for each iteration.

2.4. Ab Initio Methods. The equilibrium geometry of formaldehyde was obtained using MP2 with a cc-pvtz basis set. The excitation energy calculations of free and aqueous formaldehyde were carried out at the MRCI level using orbitals from a state-averaged multiconfigurational self-consistent field (SA-MCSCF) procedure. In most calculations the complete active space (CAS), for both the MCSCF and MRCI expansions, consists of the (π, n_O,π^*) molecular orbitals (MOs) with 4 electrons, denoted as (4,3). At the MRCI level the (1σ($1s_O$), 2σ($1s_C$)) MOs were frozen, while the (3σ, 4σ, 5σ, 6σ) MOs were doubly occupied, and single and double excitations were allowed from these orbitals into the virtual orbitals. To test the dependence of the solvatochromic shift on the active space a different CAS was used in one case. This consisted of 6 electrons in 4 orbitals, (6,4) where the four orbitals were (6 σ, π, n_O, π^*). An active space including σ orbitals has been found important in previous studies for the description of higher excited states of formaldehyde.[64] Three different basis sets were used here: the triple-ζ plus polarization (cc-pvtz) of Dunning,[65] the cc-pvtz with the addition of diffuse functions (aug-cc-pvtz),[66] and a double-ζ with polarization and diffuse functions (6-31++G**).[67] The Gaussian suite of programs[55] was used for the MP2 calculations and COLUMBUS[39−42] for all other calculations.

TABLE 2: Gas-Phase Vertical Excitation Energies to the S_1 State, T_e, and Dipole Moments at Various Levels of Theory[a]

basis set	method	T_e (eV)	μ_g(D)	μ_e(D)
cc-pvtz	MCSCF	3.97	2.25	1.23
	MRCI	4.04	2.34 (2.31)	1.33 (1.37)
6-31++G**	MCSCF	3.98	2.37	1.38
	MRCI	4.09	2.48 (2.47)	1.50 (1.52)
aug-cc-pvtz	MCSCF	3.94	2.27	1.19
	MRCI	4.01	2.41(2.41)	1.28 (1.30)
cc-pvtz (6,4)	MCSCF	3.88	2.25	1.31
	MRCI	3.99	2.34 (2.31)	1.43 (1.41)
exp[70−72]		4.07	2.33	1.57

[a] The dipole moments of the ground state, μ_g, and the excited state, μ_e, are shown. In parentheses the dipole moments calculated using response theory are given.

3. Results and Discussion

3.1. QM Calculations of Free Formaldehyde. The calculated ground-state geometry of formaldehyde is R(CO) = 1.210 Å, R(CH) = 1.101 Å, ∠(OCH) = 121.9°, and ∠(HCH) = 116.1° which shows good agreement with experiment results.[68] Table 2 shows the vertical excitation energies and dipole moments calculated at that geometry using different basis sets and active spaces. Both MCSCF and MRCI results are shown. As already discussed in the previous section three basis sets are used, cc-pvtz, aug-cc-pvtz, and 6-31++G**, with a (4,3) active space. A different active space (6,4) was also tested using the cc-pvtz basis set. The dipole moments at the MRCI level are calculated in two ways, as expectation values and using response theory.[69] The values calculated using response theory are given in parentheses in Table 2. In the limit of full-CI both ways of computing the property will give the same value, while for a "good" CI wave function the differences in the two approaches will be small. Inspection of the dipole moments in Table 2 shows small differences for our expansions. The experimental value of the excitation energy is 4.07 eV[70] which is in good agreement with our results. All the basis sets and active spaces give good vertical excitation energies, although the cc-pvtz and 6-31++G** basis sets combined with MRCI give the best agreement with experimental results. The excitation energy at the MRCI/cc-pvtz level is 4.04 eV and at the MRCI/6-31++G** level 4.09 eV, differing by 0.02−0.03 eV from the experimental value. The calculated dipole moments for the ground and excited states are also in very good agreement with experimental values. The experimentally determined dipole

TABLE 3: Calculated Dipole Moments, μ, and Induced Dipole Moments, $\Delta\mu$ (in Debye), of the Ground State and First Excited State of Formaldehyde in Aqueous Phase

μ_g(aq)	μ_e(aq)	$\Delta\mu_g$	$\Delta\mu_e$	method	ref
3.377	2.306	1.269	0.982	CASSCF/MC	50
3.442/3.662[a]	2.270/2.455[a]	1.206/1.426[a]	1.305/1.490[a]	CC2/MM	20
3.597/3.816[a]	2.500/2.683[a]	1.187/1.406[a]	1.237/1.420[a]	CCSD/MM	20
3.34	1.99	0.98	0.64	CASSCF/RISM-SCF	32
3.00	1.74	0.65	0.52	CASSCF/ASEP	19
2.637	1.822	0.247	0.353	MCSCF/PCM	47
2.932	1.999	0.570	0.447	MRCI/PCM	47
2.898	1.736	0.488	0.473	CCSD/DC	20
2.98, (3.05[b])	1.66, (1.76[b])	0.54 (0.61[b])	0.38 (0.48[b])	MRCI/COSMO	48
2.78	1.68	0.53	0.45	MCSCF(4, 3)/cc-pvtz	this work
2.89	1.83	0.56	0.50	MRCI(4, 3)/cc-pvtz	this work
2.56	1.62	0.31	0.31	MCSCF(6, 4)/cc-pvtz	this work
2.88	1.94	0.55	0.51	MRCISD(6, 4)/cc-pvtz	this work
2.91	1.78	0.64	0.59	MCSCF/aug-cc-pvtz	this work
3.09	1.95	0.68	0.67	MRCI/aug-cc-pvtz	this work
3.07	1.96	0.69	0.58	MCSCF/6-31++G**	this work
3.23	2.17	0.75	0.67	MRCI/6-31++G**	this work

[a] TIP3P/SPCpol. [b] Using solvent optimized MCSCF orbitals.

moment of the ground state is 2.33 D[71] which is in excellent agreement with the calculated cc-pvtz MRCI values. The experimentally determined dipole moment for the excited state is 1.57 D[72] which is in general 0.1−0.3 D larger than the MRCI values at vertical excitation, but the difference reflects the fact that the experimental value refers to the relaxed geometry of the excited state at its minimum. When the geometry of the excited state is minimized, using the cc-pvtz basis set and (4,3) MRCI expansion, the calculated dipole moment at the relaxed geometry increases from 1.33 to 1.48 D, in much better agreement with experiment. The adiabatic excitation energy at this level is 3.56 eV, also in very good agreement with the experimental value of 3.50 eV.[73] Overall the electronic structure results provide an excellent description of the properties of gas-phase formaldehyde. The cc-pvtz and 6-31++G** basis sets combined with MRCI give the best agreement with experimental results. Diffuse functions do not play a big role in the calculated gas-phase properties, but they play a more important role in the corresponding properties in solution as will be discussed later.

To continue with the studies in solution we used the ESPCHG program to derive the atomic charges. The dipole moment was also calculated using the derived charges and the formaldehyde geometry in order to check how well the charges can reproduce the ab initio dipole moments. These charges and dipole moments at the different levels are given in Table 1. One can see the values depend on the quality of the wave functions, and electron correlation and basis sets play an important role in the calculation of MESP and atomic charges. Comparison of the above derived dipoles with the ab initio calculated dipoles (shown in Table 2) shows that the code ESPCHG and the derived charges work well to reproduce the electrostatic distribution of the molecule.

3.2. Structural Results/Molecular Dynamics. The solvent structure is characterized by the radial distribution functions (RDF) of O(H_2CO) − H(H_2O) and O(H_2CO) − O(H_2O). The results based on the data from the MD simulation using the 6-31++G** basis set are given here explicitly and compared with other simulations. For the RDF of O(H_2CO) − H(H_2O), the first sharp peak is located around 1.75 Å, while the second peak is at 4.45 Å, and between these peaks there is a left shoulder of the second peak. For the RDF of O(H_2CO) − O(H_2O), the first sharp peak is located around 2.75 Å and the second peak at 4.35 Å. These results indicate that the solvent has two shells. The first shell is formed by the hydrogen bonding between carbonyl O of the solute and water H, with a bond lengh of 1.75 Å. The analysis of RDF suggests that there is an almost linear hydrogen bond between formaldehyde oxygen and water hydrogen. These RDFs are similar to those reported previously for aqueous formaldehyde.[20,44,50] Compared with Kongsted et al.,[20] for example, the first peaks in both RDFs here are slightly shifted outward and are more weak in strength. The structure of the solvent around the solute determines the solvatochromic shift of the excited state. As will be seen in section 3.7 the different RDFs between our work and that of Kongsted et al.[20] result in our blueshift being smaller.

It is obvious that the RDF reflects the field strength. The atomic charges and van der Waals radii of oxygen of the carbonyl group play an important role. More negative atomic charges and/or smaller van der Waals radii yield stronger hydrogen bonding and result in more hydration, reflected in a higher first peak in RDF appearing at shorter disctance. This higher degree of hydration then produces greater blueshift. When the solute polarizability is included, the atomic charges used in the MD simulation are obtained in the presence of the solvent perturbation. As a result the solvent structure changes in each cycle of the self-consistent process. Here the solute polarizability increased the partial charges, and this increase caused an increase of the height of the first peak and shift of its position to smaller distances.

3.3. Dipole Moments and Solvent Shifts. The dipole moment is calculated by

$$\mu = \mathrm{Tr}\gamma\mathbf{[r]} + \sum_A Z_A R_A \tag{11}$$

where **[r]** is the matrix of one electron *x*, *y*, *z* integrals over molecular orbitals, $\langle\phi_p|\mathbf{r}|\phi_q\rangle$, and γ is the one electron density matrix as defined in eq 9. In the case of response theory γ is an effective density matrix.[69] If the solute geometry is kept constant in the solvent, then the induced dipole moment is defined by

$$\Delta\mu^{(i)} = \mathrm{Tr}[\boldsymbol{\gamma}^{(i)}\mathbf{[r]} - \boldsymbol{\gamma}^{(i)0}[\mathbf{r}]^0] \tag{12}$$

where the superscript (*i*) denotes the state *i*, and 0 is used for the gas phase. The calculated dipole moment magnitudes for the ground and first-excited state of formaldehyde in the aqueous phase are given in Table 3. For comparison the table lists results from the literature calculated using different methods. The gas-phase dipole moment magnitudes are given in Table 2. Note

that the dipole moment of the excited state is much smaller (by 0.94−1.08 D in MCSCF, 0.90−1.13 D in MRCI) than that of the ground state, which has an important implication on the solvent effect. In the $n_O \rightarrow \pi^*$ transition in formaldehyde, an electron transfers from the carbonyl oxygen lone pair into the antibonding π^* orbital, localized above and beneath the molecular plane. This excitation leads to a reduction of the dipole moment of the molecule, and consequently, a different solvation of the electronic ground and excited states will occur. Since the dipole moment decreases from the ground state to the first excited state, the solute is more favorably solvated in the ground state which becomes more stabilized relative to the excited state. As a result the electronic excitation energy increases.

The dipole moment of formaldehyde increases upon solvation. The induced dipole moments for both ground and excited states are shown in Table 3. They are 0.5−0.8 D, and the induced dipole moment for the ground state is predicted to be slightly larger than the one of the excited state in all of our results. Most other methods predict the same trend except a QM/MM approach using coupled cluster[20] and a polarized continuum model using MCSCF,[47] which predict the excited state induced dipole moment slightly larger. The induced dipole moment is related to the polarizability of each electronic state. Jonsson et al.[74] calculated the ground- and excited-state polarizabilities and found the excited state slightly larger ($\alpha_g = 17$ au^3 and $\alpha_e = 20$ au^3). These values would support a larger induced dipole moment for the excited state.

3.3.1. Effect of ab Initio Methods. The induced dipole moments in an aqueous phase calculated at the MRCI level are larger in magnitude than those at the MCSCF level. This is a result of electron correlation (dynamic, inter- and intramolecular) being important for the description of the polarizability of formaldehyde. The effect is only 0.02−0.06 D in the small active space (4,3) but becomes ca. 0.2 D in the (6,4) active space, which indicates that the polarizability is much more sensitive to the active space than are the excitation energies. The induced dipole moments in aqueous phase are even further increased when diffuse functions are used in the basis set. The effect of diffuse functions is stronger than that of electron correlation causing the induced dipoles to increase by ca. 0.2 D.

3.4. Excitation Energy Shifts. The MRCI energies are calculated according to

$$E = \langle \Psi^{\mathrm{MRCI}} | \hat{H}_{\mathrm{QM}} + \hat{H}_{\mathrm{QM/MM}} | \Psi^{\mathrm{MRCI}} \rangle = \mathrm{Tr}\boldsymbol{\gamma}\mathbf{h}^{\mathbf{eff}} + \frac{1}{2}\sum_{pqrs} \Gamma_{\mathrm{pqrs}} \langle pq|\, rs\rangle + E^{\mathrm{nel}} \quad (13)$$

where

$$\hat{h}^{\mathrm{eff}} = \hat{h} + \sum_X \frac{Q_X}{|R_X - r|}$$

The two-electron reduced density matrix has elements

$$\Gamma_{\mathrm{pqrs}} = \sum_{IJ} c_I c_J \langle \Phi_I |\, \hat{E}_{\mathrm{pq}} \hat{E}_{\mathrm{rs}} - \delta_{\mathrm{qr}} \hat{E}_{\mathrm{ps}} | \Phi_J \rangle \quad (14)$$

The term E^{nel} does not depend on the electronic coordinates, so it is a constant for all electronic states and it will cancel when the excitation energies are calculated. The energy shift of state i upon solvation is evaluated by $\Delta E^{(i)} = E^{(i)} - E^{(i)0}$, and the excitation energy shift between two states (1) and (2) is evaluated by

$$\delta E = \Delta E^{(2)} - \Delta E^{(1)} \quad (15)$$

$$= \mathrm{Tr}[(\boldsymbol{\gamma}^{(2)} - \boldsymbol{\gamma}^{(1)})\mathbf{h}^{\mathbf{eff}} - (\boldsymbol{\gamma}^{(2)0} - \boldsymbol{\gamma}^{(1)0})\mathbf{h}^{\mathbf{eff,\,0}}] + \frac{1}{2}\sum_{pqrs}[(\Gamma^{(2)}_{\mathrm{pqrs}} - \Gamma^{(1)}_{\mathrm{pqrs}})\langle pq|rs\rangle - (\Gamma^{(2)0}_{\mathrm{pqrs}} - \Gamma^{(1)0}_{\mathrm{pqrs}})\langle pq|\, rs\rangle^0] \quad (16)$$

Table 4 shows the blueshift of the excitation energy for the various ab initio models used in this work. It varies between 1208 and 1591 cm^{-1} depending on the ab initio level. Using the best basis set in this work, which is the aug-cc-pvtz, the blueshift is predicted to be 1581 cm^{-1} at the MCSCF level and 1502 cm^{-1} at the MRCI level.

3.4.1. Effect of ab Initio Methods. The effect of various components of the ab initio methodology on the solvatochromic shifts has been investigated in this study. MCSCF and MRCI results are given in order to investigate the effect of dynamical correlation. This effect is found to be between 75 and 80 cm^{-1} for any basis set used. Dynamic electron correlation is defined and evaluated by

$$E^{\mathrm{dyn}}_{\mathrm{corr}} = E^{\mathrm{MRCI}} - E^{\mathrm{MCSCF}} \quad (17)$$

$$= \mathrm{Tr}(\boldsymbol{\gamma}^{\mathrm{MRCI}} - \boldsymbol{\gamma}^{\mathrm{MCSCF}})\mathbf{h}^{\mathbf{eff}} + \frac{1}{2}\sum_{pqrs}(\Gamma^{\mathrm{MRCI}}_{\mathrm{pqrs}} - \Gamma^{\mathrm{MCSCF}}_{\mathrm{pqrs}})\langle pq|rs\rangle \quad (18)$$

The electron density is distorted (polarized) for each state depending on its molecular polarizability, and dynamical correlation is important for its accurate description. This effect can be seen clearly by noting that the blueshifts derived by MCSCF are larger than those derived by MRCI using the same basis sets. Since the water molecules are treated classically, of course, intermolecular dynamical correlation and dispersion is not accounted for in this work.

Note that in eq 18, $E^{\mathrm{dyn}}_{\mathrm{corr}}$ implicitly includes a term

$$\mathrm{Tr}(\boldsymbol{\gamma}^{\mathrm{MRCI}} - \boldsymbol{\gamma}^{\mathrm{MCSCF}})\left[\sum_X \frac{Q_X}{|R_X - r|}\right] \quad (19)$$

This term includes the perturbation from the solvent, and it can be seen that the effect of dynamical correlation depends on the solvent charge distribution. A solvent structure closer to the solute should produce a larger effect due to dynamical correlation. Here this dependence on the solvent structure is not observed; the effect of dynamical correlation on the blueshift is ca. 80 cm^{-1} in all cases. This may be because the solvent structure is not significantly different between the different calculations.

It should be noted that the MCSCF described well the excitation energy for formaldehyde in vacuo in all cases. In cases where the dynamical correlation plays an important role in the excitation energy, the shift may be affected more. Furthermore the charges used in the MD simulations are taken from the MRCI densities and not the MCSCF ones. So the solvent structure is the one corresponding to the MRCI ground-state charge distribution. Since the charge distribution at the MCSCF level is different, using that distribution would probably increase the differences between MCSCF and MRCI results. The dipole moment is a measure of the charge distribution obtained from the different methods. Table 3 shows the dipole moments obtained from the MCSCF and MRCI wave functions. Inspection of these results shows that the MCSCF values are ca. 0.1−0.3 D lower in the ground state, so the MCSCF charges

TABLE 4: Calculated Solvent Shift in cm^{-1} for the S_1 Excited State of Formaldehyde

ref	method	blueshift
44	SCF/QM/MM	1900
12	MNDO/QM/MMpol	1150
50	CASSCF/MC	2660
20	CC2/MM	2028/2722[a]
20	CCSD/MM	2139/2803[a]
45	SCF/EHP/supermolecule	3150
32	CASSCF/RISM-SCF	1998
19	CASSCF/ASEP	1470
47	MCSCF/PCM	944
47	MRCI/PCM	944
20	CCSD/DC	669
48	MRCI/COSMO	1532
this work	MCSCF(4,3)/cc-pvtz	1283
this work	MRCI(4,3)/cc-pvtz	1208
this work	MCSCF(6,4)/cc-pvtz	1351
this work	MRCI(6,4)/cc-pvtz	1272
this work	MCSCF/aug-cc-pvtz	1581
this work	MRCI/aug-cc-pvtz	1502
this work	MCSCF/6-31++G**	1591
this work	MRCI/6-31++G**	1513

[a] TIP3P/SPCpol.

are in general smaller. Using those charges would probably have resulted in a less tight solvent structure and a smaller blueshift at the MCSCF level.

The basis set plays a more important role in the predicted blueshift. At the MRCI level with the (4,3) active space the blueshift is 1208 cm^{-1} using the cc-pvtz basis set, 1502 cm^{-1} using the aug-cc-pvtz basis set, and 1513 cm^{-1} using the 6-31++G** one. The effect of including diffuse functions in the basis set is very important. When augmented basis functions are used, the calculated blueshift increases by ca. 230−294 cm^{-1}. On the other hand, comparing the aug-cc-pvtz with the 6-31++G** results shows a difference of only 10 cm^{-1}. Although the diffuse functions are very important for the solvation effect, the size of the basis set is less important. Kongsted and co-workers have observed an increase of ca. 500 cm^{-1} when changing from an 6-31++G basis set to the aug-cc-pvtz.[20] The 6-31++G basis set does not include polarization functions and is of lower quality than any basis set used in this work. This may be the reason the effect observed in that work is larger than the basis set effect observed here.

The importance of diffuse functions in the excitation energy shifts can be an indication of diffuse character in the electronic state. The expectation values of $\langle r^2 \rangle$ have been computed for the ground and excited states in the gas phase and solution as a measure of the diffuse character in these states. At the MRCI-(4,3)/cc-pvtz level the gas-phase ground state has $\langle r^2 \rangle = 52$ au and the excited state 51 au. The solvated corresponding values are 60 au and 62 au, respectively. The 6-31++G** basis set gave very similar values. These values suggest that both ground and excited states are not very diffuse, but they become a little more diffuse when they are solvated. This small increase may be responsible for the importance of diffuse functions.

Two different MRCI expansions were used as well, one with an active space of (6,4) and another of (4,3). The blueshift is 1272 cm^{-1} when the larger (6,4) expansion is used compared to 1208 cm^{-1} with the smaller. The effect of the larger active space gives a small change, increasing the shift by 64 cm^{-1}.

3.5. Effect of Mulliken Charges. A good force field is essential to reproduce the correct solvent structure around the solute and thus the solvatochromic shift. The parameters being changed in the force field in this work are the partial charges on the atoms. The easiest way to get partial charges from quantum mechanical calculations is from a Mulliken population analysis. Mulliken charges are known to be basis set dependent and not always reliable for representing the charge distribution of the molecule. Nevertheless, they are very convenient to obtain, so knowing how well they can reproduce the solvatochromic shift can be useful for future studies. Their effect on the solvatochromic shift was explored by employing Mulliken charges in the molecular dynamics simulation. The Mulliken charges taken from the in vacuo calculations for the different basis sets employed in this work were similar except when the aug-cc-pvtz basis set was used, in which case the charges were too large. The solvation study was performed using the Mulliken charges produced from the 6-31++G** basis set calulations. Initially the charges in gas-phase formaldehyde were $Q_C = 0.107$, $Q_O = -0.241$, and $Q_H = 0.067$, and finally using the coupled procedure to polarize the solute they changed to $Q_C = 0.184$, $Q_O = -0.398$, and $Q_H = 0.107$ in the statistically converged phase. The initial blueshift is 525 cm^{-1} at the MCSCF level and 485 cm^{-1} at the MRCI level. The final blueshift is 1139 cm^{-1} at the MCSCF level and 1064 cm^{-1} at the MRCI level. This set of charges greatly underestimates the blueshift compared with that obtained from atomic charges derived from the electrostatic potential, which is 1513 cm^{-1} using the same basis set. Furthermore the effect of solute polarization is more important here since it increases the shift by more than a factor of 2. We expect that the other basis sets would give similar results, except the aug-cc-pvtz which would probably give unreasonable results, because of the Mulliken charges being too large.

A measure of how well Mulliken charges can reproduce the charge density of the molecule is the dipole moment calculated using these charges. For formaldehyde the above charges give a dipole moment for the ground state $\mu_g^\circ = 1.78$ D, while after solvation the dipole moment becomes $\mu_g(aq) = 2.62$ D. The ab initio dipole moment for gas-phase formaldehyde at this level is 2.37 D which is 0.6 D larger than what the Mulliken charges predict. This difference provides an indication that the charges underestimate the charge distribution of the molecule, and they will underestimate the electrostatic effects with the solvent. The ab initio dipoles (in unit of D) of H_2CO in water when the MD was run using Mulliken charges are as follows: 2.62 for ground state and 1.59 for the first excited state at the MCSCF/6-31++G** level and 2.75 for ground state and 1.73 for the first excited state at the MRCI/6-31++G** level. Although they are in good agreement with each other, they are smaller than the dipole moments when MESP derived charges are used (see Tables 2 and 3). It is interesting also to notice that the difference between the dipole moment calculated from the charges after solvation (2.62 D) and the corresponding ab initio dipole moment (2.75 D) is only 0.12 D, much smaller than the corresponding difference in the gas phase. Thus, the Mulliken charges in solvated formaldehyde describe the charge distribution better than the ones in free formaldehyde.

3.6. Effect of Solute Polarization. In this work the solute charge distribution is polarized since the charges are converged in the presence of the solvent. The effect of solute polarization on the solvatochromic shift can be tested by examining the blueshift at the first iteration where the charges are those of the solute in vacuo. The initial charges using the 6-31++G** basis set were $Q_C = 0.468$, $Q_O = -0.440$, and $Q_H = -0.014$ with a dipole moment of 2.48 D, while the final charges were $Q_C = 0.566$, $Q_O = -0.554$, $Q_H = -0.006$ with a dipole moment 3.183 D. The blueshift produced from the initial charge distribution of the solute using the 6-31++G** basis set at the MRCI level

is 1123 cm^{-1}, about 390 cm^{-1} smaller than the blueshift after solute polarization has been accounted for. When the aug-cc-pvtz basis set is used, the initial shift is 971 cm^{-1}, while the final is 1502 cm^{-1}, giving an even larger contribution from the solute polarization (531 cm^{-1}). These values reflect the importance of the polarizability of the solute. For molecules with larger polarizability than formaldehyde this effect is expected to be even more important in the theoretical estimation of solvatochromic shifts.

3.7. Comparison with other Theoretical and Experimental Results. The direct comparison between calculated and experimental results is not easy. The experimental blueshift for formaldehyde is uncertain because of the formation of oligomers in solution.[75] The value is believed to be between 600 and 1900 cm^{-1}, where the latter is the blueshift observed in acetone.

The excitation energy shift in solution for formaldehyde has been studied extensively using a variety of solvation models. Table 4 gives a list of theoretically obtained blueshifts. Various discrete MD calculations have been performed using a variety of quantum mechanical wave functions. In 1989 Blair et al.[44] obtained a blueshift of 1900 cm^{-1} using SCF combined with MD simulations. Later Thompson[12] got a blueshift of 1150 cm^{-1} using a semiempirical method (MNDO) and a polarizable force field, QM/MMpol. More recently more sophisticated methods have been used for the quantum description of the solute. Kawashima et al.[50] obtained 2660 cm^{-1} using an MCSCF method combined with MC simulations. As pointed out by them, the shift is probably overestimated due to the neglect of dynamical correlation in the MCSCF method. Recently, Kongsted et al.[20] used coupled clusters (CCSD) and the approximate singles and doubles coupled cluster (CC2) combined with MD simulations. They obtained a blueshift of 2139 ± 45 cm^{-1} in a nonpolarized solvent model (TIP3P) and 2803 ± 46 cm^{-1} when the solvent was polarized (SPCpol) in the CCSD/MM model with a aug-cc-pvtz basis set. The CC2/MM model reduced the shift by ca. 100 cm^{-1}. A supermolecular approach using SCF wave functions and three water molecules by Fukunaga and Morokuma[45] obtained 3150 cm^{-1}.

A number of average methods have also been used for calculating the blueshift. Naka et al.[32] obtained a blueshift of 1998 cm^{-1} using the reference interaction site model at the CASSCF level. The ASEP-MD method which is in principle the same approach as the one used here has been used with CASSCF wave functions for the blueshift in formaldehyde and gives 1470 cm^{-1}.[19] The main difference in that approach and the one presented here is that they considered the polarization of the solvent, and they did not include dynamical correlation in the quantum mechanical calculations.

Dielectric continuum studies have been performed as well. Menucci et al.[47] obtained a blueshift of 944 cm^{-1} using the polarized continuum model PCM for both MCSCF and MRCI wave functions. An MRCI study using the COSMO solvation model, that has recently been implemented in the COLUMBUS suite of programs, gave a blueshift of 1532 cm^{-1}.[48] Zazza et al.[76] have used a PCM model combined with explicit water molecules and TDDFT theory to calculate the solvatochromic shift. They also explored the dependence of the results on the basis sets. These results do not show much dependence on the basis set but a strong dependence on the number of explicit water molecules used. When no water molecules are used, the shift is ca. 500 cm^{-1}, and it increases with the addition of water molecules. When two water molecules are used, the shift is ca. 1200 cm^{-1}, and when 8 are used, it further increases to 2220 cm^{-1}.

These comparisons suggest that the continuum models usually underestimate the solvatochromic shifts. On the other hand, the supermolecular approach with only a few explicit water molecules overestimates the shift. Explicit QM/MM models predict values between 1100 and 2800 cm^{-1} depending on the quantum mechanical methods and the force field used. Induced dipole moments shown in Table 3 correlate with the predicted solvatochromic shifts. When induced dipole values are large, the solvatochromic shift is large as well, indicating a larger perturbation of the solute due to the solvent. Methods that include the polarizability of the solvent predict larger induced dipole moments and solvatochromic shifts compared to those predicted using the same method without the solvent polarizability.

In general the different models predict solvatochromic shifts in a wide range. Our results are in the middle range of the other theoretical results and agree well with experimental results, even though not all the effects have been accounted for. The results depend on the force field and the ab initio methods and variations of those two affect the blueshifts observed.

4. Conclusions

In the present paper a method that combines MCSCF and MRCI ab initio calculations and molecular dynamics simulations for describing solvatochromic shifts is presented. The method follows the procedure of Aguilar and co-workers to average the electrostatic component of the solvent and introduce it into the quantum Hamiltonian as an extra collective effective nuclear attractive term. The MD simulations are using a classical force field where the partial atomic charges on the solute are derived from the MESP at the MRCI level. The averaged solvent electrostatic potential (ASEP) in grid points enveloping the van der Waals surface is derived and fitted to partial charges. This method has been proven effective and well suitable to describe the QM-MM systems.

The solvent effect on the $n_O \rightarrow \pi^*$ electronic transition in formaldehyde has been studied, focusing on the shifts on dipole moments and on excitation energies. Electron correlation and especially diffuse functions in the basis sets affect the excitation energy shift and the dipole moments in solution. The blueshift at the MRCI/aug-cc-pvtz is 1502 cm^{-1}. Electron dynamic correlation contributes a redshift of about 75−80 cm^{-1}, while diffuse functions increase the shift by ca. 300 cm^{-1}. Solute polarizability is an important component of the solvatochromic shift contributing about 35% of its value. The induced dipole moment for both ground and excited states is 0.7 D at the MRCI/aug-cc-pvtz level with the diffuse basis functions contributing 0.2 D. Dynamical correlation contributes 0.02−0.6 D when a small active space is used but 0.3 D with a larger active space.

The present model predicts a blueshift for formaldehyde that is within the range of theoretical results and expected experimental values. Because of the reduced number of ab initio calculations that need to be carried out, it provides an effective way to incorporate the solvation effect in the excited states using a sophisticated MRCI methodology. This model will be used in future work to investigate solvent effects on the potential energy surfaces of excited states, where MRCI methods are very reliable.

Acknowledgment. This work was supported by the National Science Foundation under Grant No. CHE-0449853 and Temple University. We thank Ron Shepard and Hans Lischka for useful comments on using response theory for dipole moments.

References and Notes

(1) Tomasi, J.; Persico, M. *Chem. Rev.* **1994**, *94*, 2027.

(2) Cramer, C. J.; Truhlar, C. J. In *Reviews in Computational Chemistry*; Lipkowitz, K. B., Boyd, D. B., Eds.; Wiley-VCH: New York, 1995; Vol. 6, p 1.
(3) Tomasi, J.; Mennucci, B.; Cammi, R. *Chem. Rev.* **2005**, *105*, 2999.
(4) Gao, J. In *Reviews in Computational Chemistry*; Lipkowitz, K. B., Boyd, D. B., Eds.; Wiley-VCH: New York, 1996; Vol. 7, p 119.
(5) Gao, J. *Acc. Chem. Res.* **1996**, *19*, 298.
(6) Orozco, M.; Luque, F. J. *Chem. Rev.* **2000**, *100*, 4187−4225.
(7) Warshel, A.; Levitt, M. *J. Mol. Biol.* **1976**, *103*, 227.
(8) Warshel, A. *J. Phys. Chem.* **1979**, *83*, 1640.
(9) Luzhkov, V.; Warshel, A. *J. Am. Chem. Soc.* **1991**, *113*, 4491.
(10) Gao, J. *J. Am. Chem. Soc.* **1994**, *116*, 9324.
(11) Thompson, M. A.; Schenter, G. K. *J. Phys. Chem.* **1995**, *99*, 6374.
(12) Thompson, M. A. *J. Phys. Chem.* **1996**, *100*, 14492.
(13) Warshel, A.; Chu, Z. T. *J. Phys. Chem. B* **2001**, *105*, 9857.
(14) Ryckaert, J.-P.; Ciccotti, G.; Berendsen, H. J. C. *J. Comput. Phys.* **1977**, *23*, 327.
(15) Andersen, C. *J. Comput. Phys.* **1983**, *52*, 24.
(16) Leach, A. R. *Molecular Modelling Principles and Applications;* Prentice Hall: Dorchester, 2001.
(17) Dupuis, M.; Aida, M.; Kawashima, Y.; Hirao, K. *J. Chem. Phys.* **2002**, *117*, 1242.
(18) Poulsen, T. D.; Kongsted, J.; Osted, A.; Ogilby, P. R.; Mikkelsen, K. V. *J. Chem. Phys.* **2001**, *115*, 2393.
(19) Martín, M. E.; Sánchez, M. L.; Olivares Del Valle, F. J.; Aguilar, M. A. *J. Chem. Phys.* **2000**, *113*, 6308.
(20) Kongsted, J.; Osted, A.; Mikkelsen, K. V.; Åstrand, P.-O.; Christiansen, O. *J. Chem. Phys.* **2004**, *121*, 8435.
(21) Jørgensen, P.; Simons, J. *J. Chem. Phys.* **1983**, *79*, 334.
(22) Page, M.; Saxe, P.; Adams, G. F.; Lengsfield, B. H. *J. Chem. Phys.* **1984**, *81*, 434.
(23) Helgaker, T.; Almlöf, J. *Int. J. Quantum Chem.* **1984**, *26*, 275.
(24) Shepard, R. In *Modern Electronic Structure Theory Part I*; Yarkony, D. R., Ed.; World Scientific: Singapore, 1995; p 345.
(25) Lischka, H.; Dallos, M.; Shepard, R. *Mol. Phys.* **2002**, *100*, 1647.
(26) Lischka, H.; Dallos, M.; Szalay, P. G.; Yarkony, D. R.; Shepard, R. *J. Chem. Phys.* **2004**, *120*, 7322.
(27) Dallos, M.; Lischka, H.; Shepard, R.; Yarkony, D. R.; Szalay, P. G. *J. Chem. Phys.* **2004**, *120*, 7330.
(28) Matsika, S.; Yarkony, D. R. *J. Chem. Phys.* **2002**, *117*, 6907.
(29) Matsika, S. *J. Phys. Chem. A* **2004**, *108*, 7584−7590.
(30) Ten-no, S.; Hirata, F.; Kato, S. *Chem. Phys. Lett.* **1993**, *214*, 391.
(31) Ten-no, S.; Hirata, F.; Kato, S. *J. Chem. Phys.* **1994**, *100*, 7443.
(32) Naka, K.; Morita, A.; Kato, S. *J. Chem. Phys.* **1999**, *110*, 3484.
(33) Naka, K.; Sato, H.; Morita, A.; Hirata, F.; Kato, S. *Theor. Chem. Acc.* **1999**, *102*, 165.
(34) Sánchez, M. L.; Aguilar, M. A.; Olivares del Valle, F. J. *J. Comput. Chem.* **1997**, *18*, 313.
(35) Sánchez, M. L.; Martín, M. E.; Aguilar, M. A.; Olivares del Valle, F. J. *Chem. Phys. Lett.* **1999**, *310*, 1995.
(36) Sánchez, M. L.; Aguilar, M. A.; Olivares del Valle, F. J. *J. Mol. Struct.(THEOCHEM)* **1997**, *426*, 181.
(37) Fdez. Galván, I.; Sánchez, M. L.; Martín, M. E.; Olivares del Valle, F.; Aguilar, M. *J. Chem. Phys.* **2000**, *21*, 705.
(38) Sánchez, M. L.; Martín, M. E.; Aguilar, M.; Olivares del Valle, F. *J. Comput. Chem.* **2000**, *21*, 705.
(39) Lischka, H.; Shepard, R.; Brown, F. B.; Shavitt, I. *Int. J. Quantum Chem. Sump.* **1981**, *15*, 91−100.
(40) Shepard, R.; Shavitt, I.; Pitzer, R. M.; Comeau, D. C.; Pepper, M.; Lischka, H.; Szalay, P. G.; Ahlrichs, R.; Brown, F. B.; Zhao, J. *Int. J. Quantum Chem., Quantum Chem. Symp.* **1988**, *22*, 149.
(41) Lischka, H.; Shepard, R.; Pitzer, R. M.; Shavitt, I.; Dallos, M.; Müller, T.; Szalay, P. G.; Seth, M.; Kedziora, G. S.; Yabushita, S.; Zhang, Z. *Phys. Chem. Chem. Phys.* **2001**, *3*, 664.
(42) *COLUMBUS, an ab initio electronic structure program, release 5.9.1*; Lischka, H.; Shepard, R.; Shavitt, I.; Pitzer, R. M.; Dallos, M.; Müller, T.; Szalay, P. G.; Brown, F. B.; Ahlrichs, R.; Böhm, H. J.; Chang, A.; Comeau, D. C.; Gdanitz, R.; Dachsel, H.; Ehrhardt, C.; Ernzerhof, M.; Hchtl, P.; Irle, S.; Kedziora, G.; Kovar, T.; Parasuk, V.; Pepper, M. J. M.; Scharf, P.; Schiffer, H.; Schindler, M.; Schüler, M.; Seth, M.; Stahlberg, E. A.; Zhao, J.-G.; Yabushita, S.; Zhang, Z.; Barbatti, M.; Matsika, S.; Schuurmann, M.; Yarkony, D. R.; Brozell, S. R.; Beck, E. V.; Blaudeau, J.-P. 2006.
(43) Ponder, J. *TINKER − Software Tools for Molecular Design, Version 4.2;* J. William Ponder: 2004.
(44) Blair, J. T.; Krogh Jespersen, K.; Levy, R. M. *J. Am. Chem. Soc.* **1989**, *111*, 6948.
(45) Fukunaga, H.; Morokuma, K. *J. Phys. Chem.* **1993**, *97*, 59.
(46) Bader, J. M.; Cortis, C. M.; Berne, B. J. *J. Chem. Phys.* **1997**, *106*, 2372.
(47) Menucci, B.; Cammi, R.; Tomasi, J. *J. Chem. Phys.* **1998**, *109*, 2798.
(48) Andrade do Monte, S.; Müller, T.; Dallos, M.; Lischka, H.; Diedenhofen, M.; Klamt, A. *Theor. Chem. Acc.* **2004**, *111*, 78.
(49) Dupuis, M.; Kawashima, Y.; Hirao, K. *J. Chem. Phys.* **2002**, *117*, 1256.
(50) Kawashima, Y.; Dupuis, M.; Hirao, K. *J. Chem. Phys.* **2002**, *117*, 248.
(51) Chirlian, L. E.; Francl, M. M. *J. Comput. Chem.* **1987**, *8*, 894.
(52) Breneman, C. M.; Wiberg, K. B. *J. Comput. Chem.* **1990**, *11*, 361.
(53) Shavitt, I. In *Methods of Electronic Structure Theory*; Schaefer, H. F., III, Ed.; Plenum Press: New York, 1977; Vol. 4 of *Modern Theoretical Chemistry*, pp 189−275.
(54) Williams, D. E. In *Reviews in Computational Chemistry*; Lipkowitz, K. B., Boyd, D. B., Eds.; VCH Publishers. Inc.: New York, 1991; Vol. 2, p 219.
(55) *Gaussian 03, Revision C.02*; Frisch, M. J.; Trucks, G. W.; Schlegel, H. B.; Scuseria, G. E.; Robb, M. A.; Cheeseman, J. R.; Montgomery, J. A., Jr.; Vreven, T.; Kudin, K. N.; Burant, J. C.; Millam, J. M.; Iyengar, S. S.; Tomasi, J.; Barone, V.; Mennucci, B.; Cossi, M.; Scalmani, G.; Rega, N.; Petersson, G. A.; Nakatsuji, H.; Hada, M.; Ehara, M.; Toyota, K.; Fukuda, R.; Hasegawa, J.; Ishida, M.; Nakajima, T.; Honda, Y.; Kitao, O.; Nakai, H.; Klene, M.; Li, X.; Knox, J. E.; Hratchian, H. P.; Cross, J. B.; Bakken, V.; Adamo, C.; Jaramillo, J.; Gomperts, R.; Stratmann, R. E.; Yazyev, O.; Austin, A. J.; Cammi, R.; Pomelli, C.; Ochterski, J. W.; Ayala, P. Y.; Morokuma, K.; Voth, G. A.; Salvador, P.; Dannenberg, J. J.; Zakrzewski, V. G.; Dapprich, S.; Daniels, A. D.; Strain, M. C.; Farkas, O.; Malick, D. K.; Rabuck, A. D.; Raghavachari, K.; Foresman, J. B.; Ortiz, J. V.; Cui, Q.; Baboul, A. G.; Clifford, S.; Cioslowski, J.; Stefanov, B. B.; Liu, G.; Liashenko, A.; Piskorz, P.; Komaromi, I.; Martin, R. L.; Fox, D. J.; Keith, T.; Al Laham, M. A.; Peng, C. Y.; Nanayakkara, A.; Challacombe, M.; And B. Johnson, P. M. W. G.; Chen, W.; Wong, M. W.; Gonzalez, C.; Pople, J. A. 2004.
(56) Hockney, R. W.; Eastwood, J. W. *Computer Simulation Using Pareticles;* McGraw-Hill: New York, 1981.
(57) Darden, T.; York, D.; Pedersen, L. G. *J. Chem. Phys.* **1993**, *98*, 10089−10092.
(58) Essmann, U.; Perera, L.; Berkowitz, M.; Darden, T.; Lee, H.; Pedersen, L. G. *J. Chem. Phys.* **1995**, *103*, 8577.
(59) Turner, P. H.; Cox, A. P. *Chem. Soc. J. Faraday Trans., Part II, Chem. Phys.* **1978**, *74*, 533.
(60) Weiner, S. J.; Kollman, P. A.; Case, D. A.; Singh, U. C.; Ghio, C.; Alagona, G.; Profeta, S., Jr.; Weiner, P. *J. Am. Chem. Soc.* **1984**, *106*, 765.
(61) Miertus, S.; Bartos, J.; Trebaticka, M. *J. Mol. Liq.* **1987**, *33*, 139.
(62) Badenhoop, J. K.; Weinhold, F. *J. Chem. Phys.* **1997**, *107*, 5422.
(63) Allen, M.; Tildesley, D. *Computer Simulation of Liquids;* Clarendon: Oxford, 1987.
(64) Dallos, M.; Müller, T.; Lischka, H.; Shepard, R. *J. Chem. Phys.* **2001**, *114*, 746−757.
(65) Dunning, T. H., Jr. *J. Chem. Phys.* **1989**, *90*, 1007.
(66) Dunning, T. H., Jr.; Hay, P. J. In *Methods of Electronic Structure Theory*; Schaefer, H. F., III, Ed.; Plenum Press: New York and London, 1977; pp 1−27.
(67) Krishnan, R.; Binkley, J. S.; Seeger, R.; Pople, J. A. *J. Chem. Phys.* **1980**, *72*, 650.
(68) Yamada, K.; Nakagawa, T.; Kuchitsu, K.; Morino, Y. *J. Mol. Spectrosc.* **1971**, *38*, 70.
(69) Shepard, R.; Lischka, H.; Szalay, P. G.; Kovar, T.; Ernzerhof, M. *J. Chem. Phys.* **1992**, *96*, 2085.
(70) Robin, M. B. *Higher Excited States of Polyatomic Molecules*; Academic: New York, 1985; Vol. III.
(71) Kondol, K.; Oka, T. *J. Phys. Soc. Jpn.* **1960**, *15*, 307.
(72) Freeman, D. E.; Klemperer, W. *J. Chem. Phys.* **1966**, *45*, 52.
(73) Clouthier, D. J.; Ramsay, D. A. *Annu. Rev. Phys. Chem.* **1983**, *34*, 31.
(74) Jonsson, D.; Norman, P.; Agren, H. *Chem. Phys.* **1997**, *224*, 201−214.
(75) Bercovici, T.; King, J.; Becker, R. S. *J. Chem. Phys.* **1972**, *56*, 3956.
(76) Zazza, C.; Bencivenni, L.; Grandi, A.; Aschi, M. *J. Mol. Struct.* **2004**, *680*, 117.